AGU PUBLICATIONS

JGR

Journal of Geophysical Research: Space Physics

RESEARCH ARTICLE

10.1002/2013JA019253

Key Points:
- Spectra and pitch angle distributions of SEPs reconstructed for the GLE 71
- Different populations of particles are found, and their origin is speculated
- A sunward SEP population is explained by a preexisting magnetic mirror

Supporting Information:
- Readme
- Animation S1
- Animation S2

Correspondence to:
I. G. Usoskin,
Ilya.Usoskin@oulu.fi

Citation:
Mishev, A. L., L. G. Kocharov, and I. G. Usoskin (2014), Analysis of the ground level enhancement on 17 May 2012 using data from the global neutron monitor network, *J. Geophys. Res. Space Physics*, *119*, 670–679, doi:10.1002/2013JA019253.

Received 25 JUL 2013
Accepted 11 JAN 2014
Accepted article online 17 JAN 2014
Published online 11 FEB 2014

Analysis of the ground level enhancement on 17 May 2012 using data from the global neutron monitor network

A. L. Mishev[1,2], L. G. Kocharov[1], and I. G. Usoskin[1,3]

[1]Sodankylä Geophysical Observatory (Oulu Unit), University of Oulu, Oulu, Finland, [2]Institute for Nuclear Research and Nuclear Energy, Bulgarian Academy of Sciences, Sofia, Bulgaria, [3]Department of Physics, University of Oulu, Oulu, Finland

Abstract We have analyzed the data of the world neutron monitor network for the first ground level enhancement of solar cycle 24, the ground level enhancement (GLE) on 17 May 2012. A newly computed neutron monitor yield function and an inverse method are applied to estimate the energy spectrum, anisotropy axis direction, and pitch angle distribution of the high-energy solar particles in interplanetary space. The method includes the determination of the asymptotic viewing cones of neutron monitor stations through computations of trajectories of cosmic rays in a model magnetosphere. The cosmic ray particle trajectories are determined with the GEANT-based MAGNETOCOSMICS code using Tsyganenko 1989 and International Geomagnetic Reference Field models. Subsequent calculation of the neutron monitor responses with the model function is carried out, that represents an initial guess of the inverse problem. Derivation of the solar energetic particle characteristics is fulfilled by fitting the data of the global neutron monitor network using the Levenberg-Marquardt method over the nine-dimensional parameter space. The pitch angle distribution and rigidity spectrum of high-energy protons are obtained as function of time in the course of the GLE. The angular distribution appears quite complicated. It comprises a focused beam along the interplanetary magnetic field line from the Sun and a loss-cone feature around the opposite direction, possibly indicative of the particle transport in interplanetary magnetic field structures associated with previous coronal mass ejections.

1. Introduction

The Earth is constantly bombarded by high-energy particles—cosmic rays. Those primary particles, which are not deflected away by the geomagnetic field, enter the atmosphere and undergo interactions with atoms and molecules of the atmosphere. While low-energy primary particles (below ~ 450 MeV) are completely absorbed in the atmosphere and do not reach sea level, those with high energies produce new particles throughout interactions with air nuclei leading to the development of atmospheric nuclear-electromagnetic-muon cascade [e.g., *Bazilevskaya et al.*, 2008]. In such a cascade a small fraction of the energy of the initial primary particle reaches the ground as energetic secondary particles. Most of the primary particle energy is released in the atmosphere by collisions, ionization, and excitation of the air molecules, resulting in ionization of the ambient air.

Most of the primary particles are of extrasolar origin known as galactic cosmic rays (GCR). They are always present in the vicinity of Earth. Their intensity is affected by solar activity, following the 11 year solar cycle and responding to long– and short–time scale solar wind variations. Some solar flares and eruptive events, such as coronal mass ejections (CMEs), can accelerate protons and other ions to high energies [*Cliver et al.*, 2004; *Aschwanden*, 2012, and references therein]. Such solar energetic particles (SEPs) enter the atmosphere sporadically, with a greater probability during periods of high solar activity [e.g., *Shea and Smart*, 1990]. Similar to GCR cascades described above, they could lead to an increase of the intensities recorded by neutron monitors on the surface of the Earth, known as ground level enhancements (GLEs).

Analysis of the characteristics of the primary solar particles causing GLEs, such as energy spectra and anisotropy, from ground-based data records is a serious challenge [*Dorman*, 2006; *Ruffolo et al.*, 2006; *Aschwanden*, 2012]. The energy spectra and anisotropy bring crucial information for understanding the acceleration mechanisms of SEPs and their propagation in the interplanetary medium [*Debrunner et al.*, 1988; *Reames*, 1999]. A convenient instrument for the determination of the GLE characteristics is the network of standard neutron monitors (NMs), [*Simpson et al.*, 1953]. The purpose of a NM is to detect, deep

within the atmosphere, variations of the cosmic ray intensity in the interplanetary medium [*Hatton*, 1971; *Dorman*, 2004].

The trajectory of a primary cosmic ray particle that reaches the Earth's atmosphere is governed by the geomagnetic field, which results in geomagnetic cutoff rigidity varying from a minimum at the magnetic poles to a vertical cut-off rigidity of about 15 GV in the equatorial regions. In high-latitude regions, where the geomagnetic cutoff is low, the lower threshold response of the neutron monitor is controlled by the atmospheric mass which is about 1030 g cm^{-2} at sea level. This limits the response threshold of the neutron monitor to primary particles of about 430 MeV/nucleon. In regions like Central Antarctica, at the elevation of $\sim$ 3 km above sea level, the reduced atmospheric mass lowers the threshold to $\sim$ 300 MeV/nucleon. At midlatitudes or equatorial latitudes, the detection threshold is totally controlled by the geomagnetic cutoff. Neutron monitors at high altitudes have higher counting rates than those at lower altitudes because of the atmospheric attenuation of the secondary particles generated in the atmosphere, but they are sensitive to the same energy range as the corresponding sea level NMs but with slightly different spectral response [*McCracken*, 1962; *Dorman*, 2004].

Since the intensity of cosmic rays is not uniform around the Earth, it is important to place neutron monitors at multiple locations in order to obtain a complete picture of cosmic rays in space [*Bieber and Evenson*, 1995]. This is particularly important for GLEs, which typically possess an essential anisotropic part. The measurements performed by the worldwide network of NMs are used to determine the spectral and angular characteristics of SEPs near Earth causing GLEs [e.g., *Mavromichalaki et al.*, 2011]. In order to build a reconstruction method to assess the GLE characteristics, a relationship between NM count rates and the primary particle flux needs to be established. There are several crucial points: particle transport in the geomagnetosphere (an appropriate magnetospheric model), particle transport in the Earth atmosphere (direct simulation with Monte Carlo methods, theoretical computations of coupling function or yield function), and detection efficiency of NM to secondary particles (mostly neutrons and protons) [*Hatton*, 1971; *Dorman*, 2004]. In this study, we apply our recently computed NM yield function [*Mishev and Usoskin*, 2013; *Mishev et al.*, 2013] and an approach similar to that used by *Cramp et al.* [1997], *Bombardieri et al.* [2006], and *Vashenyuk et al.* [2006, 2008] (see details below). Here we demonstrate an application of the method to the analysis of the GLE on 17 May 2012.

On 17 May 2012 the active region NOAA 11476 at the Sun produced a coronal mass ejection and an associated moderately strong (class M5.1) flare at 01:25 UT. The active region was located near N07 W88, implying that the Earth was magnetically connected to the eruption core. At around 01:50 UT the worldwide NM network detected the first ground level enhancement since December 2006. The flux of particles with energy effective for NM detection, viz., above 500 MeV, remained above the GCR background for about 1 hour. The enhancement was registered by several NM stations. The highest increases in the count rates were observed at South Pole, Oulu, and Apatity NMs with the maximal count rate increase of about 22% (Figure 1). The remaining NM stations registered only moderate increase of a few percent, therefore a large anisotropy at the beginning of the event was observed.

2. Modeling the Neutron Monitor Response

Methods for modeling the neutron monitor response during a GLE have been developed over many years. In general, the standard analysis of GLE events is based on an inverse problem solution, considering data from several NM stations [*Shea and Smart*, 1982; *Cramp et al.*, 1997; *Bombardieri et al.*, 2006; *Vashenyuk et al.*, 2006, 2008]. Data from stations with different cutoff rigidities (geomagnetic latitudes) provide information necessary to determine the spectral characteristics. Responses of stations over a wide range of geographical locations are required to determine the particle anisotropy and its axis of symmetry. The pitch angle distribution (PAD) and the rigidity spectrum are determined simultaneously using a convenient optimization procedure [e.g., *Cramp et al.*, 1994, 1997]. The fractional increase of the count rate of a NM station represents the ratio between the NM count rate due to GLE and the GCR counting rate, the latter defined as an average over a complete hour before the GLE onset [*Shea et al.*, 1987]. The relative count rate increase of a given NM at given time t can be expressed as

$$\frac{\Delta N(P_{cut},t)}{N(t)} = \frac{\int_{P_{cut}}^{P_{max}} J_{||sep}(P,t)Y(P)G(\alpha(P),t)\mathrm{d}P}{\int_{P_{cut}}^{\infty} J_{GCR}(P,t)Y(P)\mathrm{d}P}, \quad (1)$$

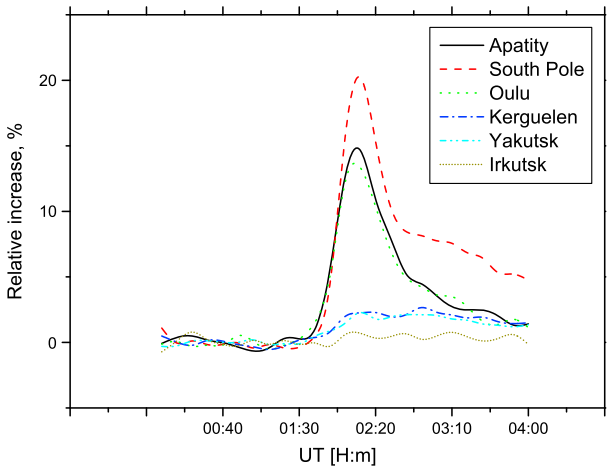

Figure 1. NM count rate enhancement for several NM stations during GLE 71 on 17 May 2012.

where $N(t)$ is the count rate due to GCR, $\Delta N(P_{cut}, t)$ is the count rate increase due to solar particles, considering all allowed trajectories (see equation (4) below), $J_{||sep}$ is the primary solar particles rigidity spectrum, $J_{GCR}(P, t)$ is the rigidity spectrum of GCR, $Y(P)$ is the NM yield function, and $G(\alpha, t)$ is the SEP pitch angle distribution. In equation (1), P_{cut} is the minimum cutoff rigidity of the station and P_{max} is the maximum rigidity considered in the model, assumed to be 20 GeV, which is sufficiently high for solar particles even in major events. We apply a parameterizations of the GCR spectrum based on the force field model [*Gleeson and Axford*, 1968; *Caballero-Lopez and Moraal*, 2004; *McCracken et al.*, 2004; *Usoskin and Kovaltsov*, 2006], using an approximation of the local interstellar spectrum [*Burger et al.*, 2000; *Usoskin et al.*, 2005], and reconstruct solar modulation parameter according to *Usoskin et al.* [2011]. A modified power law in rigidity is assumed for the spectrum of GLE-causing solar particles [cf. *Cramp et al.*, 1997; *Bombardieri et al.*, 2006; *Vashenyuk et al.*, 2008]:

$$J_{||}(P) = J_0 P^{-(\gamma+\delta\gamma(P-1))} \ , \tag{2}$$

where $J_{||}$ is the particle flux arriving from the Sun along the PAD axis of symmetry defined by geographic coordinate angles Ψ and Λ, γ is the power law spectral exponent at rigidity $P = 1$ GV, $\delta\gamma$ is the rate of the spectrum steepening. The pitch angle distribution is modeled as a superposition of two Gaussians (similar to *Cramp et al.* [1997], *Bombardieri et al.* [2006], and *Vashenyuk et al.*, 2008).

$$G(\alpha) = \exp(-\alpha^2/\sigma_1^2) + B * \exp(-(\alpha - \alpha')^2/\sigma_2^2) \ , \tag{3}$$

where α is the particle's pitch angle, σ_1 and σ_2 are the width parameters of the pitch angle distribution, and B and α' are parameters of the flux from a possible second direction. The pitch angle is defined as the angle between the asymptotic direction and the axis of anisotropy. Therefore, according to equations (1)–(3), nine model parameters have to be determined: J_0, γ, $\delta\gamma$, Ψ and Λ, α', σ_1, σ_2 and B. According to equation (3) the PAD is assumed to be azimuthally symmetric with its maximum in the forward propagation direction (away from the Sun), with zero pitch angle defined along the axis of symmetry. Equation (3) allows us to consider a bidirectional anisotropy [*Cramp et al.*, 1997], which could result from bouncing particles inside a looped magnetic field structure (magnetic bottle) [*Saiz et al.*, 2008] or by particles scattered beyond the Earth [*Bieber et al.*, 2002].

Therefore, an analysis of GLEs based on NM data consists of several consecutive steps: definition of asymptotic viewing cones of the NM stations by computation of particle trajectories in a model magnetosphere; calculation of the NM responses, i.e., an initial guess of the inverse problem; application of an optimization procedure (inverse method) for the determination of primary solar proton parameters: energy spectrum, anisotropy axis direction, and pitch angle distribution.

Access of low-energy cosmic rays to any position on the Earth depends on the state of the magnetosphere [e.g., *Kudela and Usoskin*, 2004; *Kudela et al.*, 2008]. The problem of defining the asymptotic directions for a specific NM was of great interest over the years. Several models, tools, and algorithms to calculate geomagnetic cutoff rigidities, particle trajectories, and the asymptotic viewing cones were proposed [*McCracken et al.*, 1962, 1968; *Shea et al.*, 1965; *Smart et al.*, 2000]. In the present work we consider the International Geomagnetic Reference Field (IGRF) geomagnetic model (epoch 2010) as the internal field and the Tsyganenko 89 model as the external field. This combination provides the most efficient computation of asymptotic directions [*Cramp et al.*, 1997; *Buetikofer et al.*, 2008]. The IGRF model is a mathematical model of geomagnetic field and its annual secular variation, that is mathematically described by Gauss coefficients, which define a spherical harmonic expansion of the magnetic scalar potential [*Langel*, 1987]. In fact,

it represents the most precise model of the geomagnetic field, in which the coefficients are derived from magnetic field measurements with geomagnetic stations, magnetometers, and satellites. The model by *Tsyganenko* [1989] is a semiempirical model based on a large number of satellite observations. The model takes into account the contributions from external magnetospheric sources: the ring current, the magnetotail current system, magnetopause currents, and the large-scale system of field-aligned currents. It accounts for seasonal and diurnal changes of the magnetospheric field as well as for changes in the geomagnetic activity level indicated by the *Kp* index. The Tsyganenko 89 model provides seven different states of the magnetosphere corresponding to different levels of geomagnetic activity. It is driven only by the geomagnetic activity index *Kp* and provides perfect balance between simplicity and realism [*Kudela et al.*, 2008; *Nevalainen et al.*, 2013].

Here we use asymptotic viewing cones, i.e., the set of asymptotic directions of all allowed trajectories (the arrival direction of a charged particle of specified rigidity coming from interplanetary space is allowed or forbidden if such a particle can or cannot reach a given location on the Earth through the geomagnetic field, respectively [*Cooke et al.*, 1991].) Computations of the asymptotic viewing cones and cutoff rigidities of NM stations considered for analysis are performed with GEANT 4 [*Agostinelli et al.*, 2003] based code MAGNETOCOSMICS [*Desorgher et al.*, 2005], which allows us to compute propagation of charged particles through the Earth's magnetosphere. For convenience of numerical implementation, we recast equation (1) as a sum over the nine asymptotic directions *i* and the appropriate rigidity grid:

$$\frac{\Delta N(P_{\mathrm{cut}},t)}{N(t)} = \frac{1}{9}\sum_{i(\theta,\phi)=1}^{9} \frac{\sum_{P_{\mathrm{cut}}}^{P_{\mathrm{max}}} A(P,\theta,\phi) J_{||\mathrm{sep}}(P,t) Y(P) G(\alpha(P),t) \Delta P}{\sum_{P_{\mathrm{cut}}}^{P_{\infty}} A(P,\theta,\phi) J_{\mathrm{GCR}}(P,t) Y(P) \Delta P}, \tag{4}$$

where $\Delta N(P_c, t)$ is the absolute count rate increase due to GLE, $N(t)$ is the background count rate due to GCR, P is the particle's rigidity, P_{cut} and P_{max} are the minimum and maximum rigidity of considered particles for a given station, $A(P, \theta, \phi)$ is a parameter equal to 0 and 1 for forbidden and allowed trajectories, respectively, $J_{||\mathrm{sep}}$ is the solar particle spectrum according to equation (2), J_{GCR} is the flux of GCR at 1 AU calculated for the corresponding level of solar modulation, and θ and ϕ are the zenith and azimuth angle of arriving particles. The nine directions correspond to $\theta = 0°$, 15°, and 30° and $\phi = 0°$, 90°, 180°, and 270° [*Clem*, 1997; *Cramp et al.*, 1997; *Vashenyuk et al.*, 2006]. As it was demonstrated originally by *Rao et al.* [1963], the increasing solid angle for nonvertical particle directions partly compensates the increasing mass overburden (also *Cramp et al.*, 1997; *Bombardieri et al.*, 2006). In this model we consider $P_{\mathrm{max}} = 20$ GV for each NM station and accordingly set $P_{\infty} = 1$ TV in (4) for the computation of GCR background. The summation over rigidity in (4) is performed with step size of 0.001 GV.

The optimization is performed for the difference between modeled and measured responses of *m* NM stations, i.e., minimization of the functional $\mathcal{F}$ over the vector of the nine unknown parameters described above after equation (3):

$$\mathcal{F} = \sum_{i=1}^{m} \left[\left(\frac{\Delta N_i}{N_i} \right)_{\mathrm{mod.}} - \left(\frac{\Delta N_i}{N_i} \right)_{\mathrm{meas.}} \right]^2. \tag{5}$$

For the solution of the inverse problem we apply a procedure of nonlinear optimization using the Levenberg-Marquardt algorithm (LMA) [*Levenberg*, 1944; *Marquardt*, 1963] with Minpack code [*More et al.*, 1980]. The LMA provides a numerical solution to the problem of minimizing a nonlinear function over the space of parameters of the function. The LMA interpolates between the Gauss-Newton algorithm and the method of gradient descent. The advantage of the method is that it finds a solution even if the initial guess is away from the final solution [*Dennis and Schnabel*, 1996]. During the analysis, zero excess counts from different stations are included along with data from stations with significant increases.

3. Results and Discussion

For the analysis of the GLE on 17 May 2012, we consider data from 21 different NMs around the globe (Alma Ata, Apatity, Baksan, Fort Smith, Inuvik, Irkutsk, Jungfraujoch, Kerguelen, Kiel, Magadan, McMurdo, Moscow, Norilsk, Oulu, Rome, South Pole, Terre Adelie, Thule, Tsumeb, Tixie Bay, and Yakutsk), representing the cutoff rigidity range from 0 GV to 6.12 GV. The considered NM stations allow derivation on the rigidity spectrum of GLE over the range 0.8 GV −7 GV.

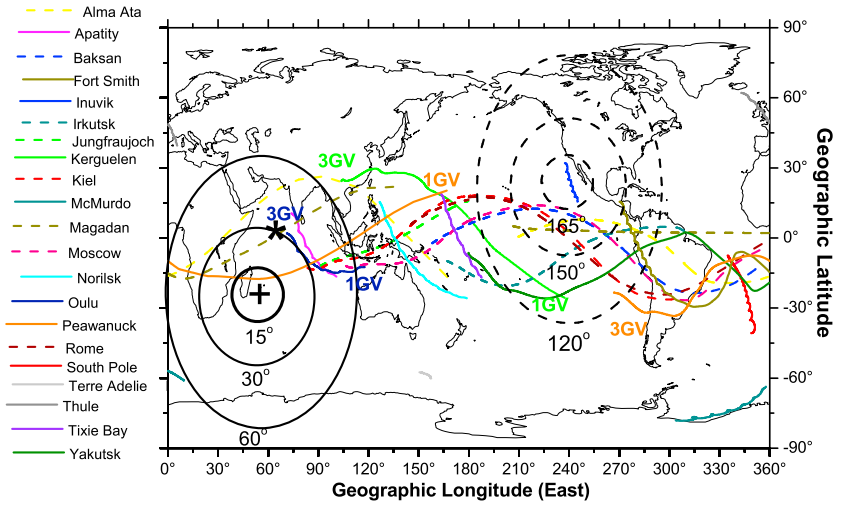

Figure 2. Calculated NM asymptotic directions during GLE 71 at 02:00 UT on 17 May 2012. The directions are for the rigidity interval from 1 GV to 3 GV for polar NMs, from R_c to 5 GV for midrigidity cutoff NMs and from R_c to 8 GV for high-rigidity cutoff NMs. The asterisk shows the direction of heliospheric magnetic field (HMF) derived from the ACE satellite measurements. The cross represents the derived apparent source position (anisotropy axis of GLE 71). The lines of equal pitch angles relative to the derived anisotropy axis are plotted for 15°, 30°, 60°, 165°, 150°, and 120°. The asymptotic directions of polar NMs are plotted with solid lines, while midlatitude NMs are plotted with dashed lines.

The NM data are retrieved from the Neutron Monitor Database (NMDB) website (http://www.nmdb.eu) [*Mavromichalaki et al.*, 2011]. We consider the 10 min averaged data for the analysis. The NM count rates are normalized to sea level applying a correction of high-altitude station responses using the two-attenuation length method [*McCracken*, 1962]. A plot of the asymptotic viewing directions of all NMs considered in our analysis is shown in Figure 2 with a sample of several selected rigidities along the asymptotic curves of Kerguelen, Peawanuck, and Oulu. Figure 2 also shows the direction of the heliospheric magnetic field (asterisk) as derived from the ACE satellite measurements as well as the derived anisotropy axis (cross). Contours of equal pitch angles relative to the derived anisotropy axis are also plotted. The time evolution of the estimated axis of symmetry of particle arrival and the heliospheric magnetic field direction measured on board the ACE satellite during the event are presented in Figure 3. The offset between the anisotropy axis and the magnetic field varies through the event by up to 30°.

The cutoff rigidity of each station has been evaluated by the backward trajectory-tracing technique [*Smart et al.*, 2000]. The neutron monitors considered here possess different asymptotic cones. A combination of different cutoff rigidities and asymptotic cones leads to different profiles of the NM count rates observed at different stations. The Oulu and Apatity NMs, which recorded a strong increase, have asymptotic directions close to each other. The South Pole NM also recorded a strong increase, while the other stations do not. More than a half of the NM stations used in this analysis are located at high latitudes. The cutoff rigidity of a high-latitude NM is determined mostly by the atmospheric absorption rather than the geomagnetic shielding. This results in nearly identical energy thresholds. Therefore, the observed differences in counting rates of different high-latitude NM stations can generally be attributed to the anisotropy of the GLE. In addition, polar NMs have greater directional sensitivity compared to midlatitude NMs [*Bieber and Evenson*, 1995].

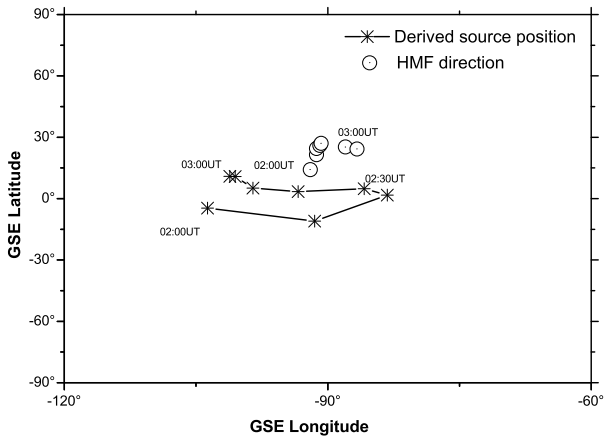

Figure 3. Derived axis of symmetry of particle arrival and heliospheric magnetic field direction as a function of time throughout the event.

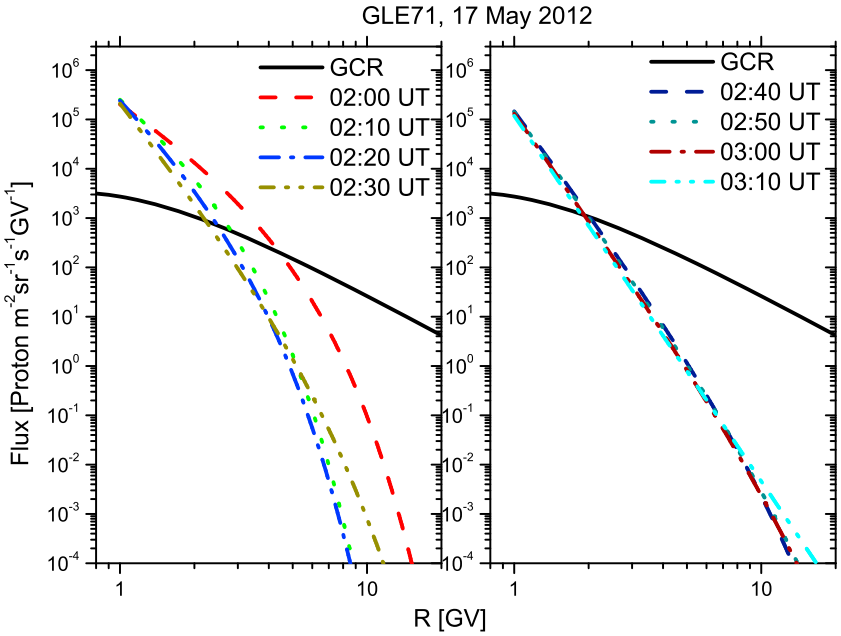

Figure 4. Derived rigidity spectra of solar high-energy particles during GLE 71 for eight successive 10 min intervals. Plotted is the particle flux along the symmetry axis, $J_{\|sep}$ in equation (4). Time (UT) refers to the start of the corresponding 10 min interval.

The GLE on 17 May 2012 had a hard rigidity spectrum and a strong anisotropy. This is specifically demonstrated by the sharp pulse-like enhancement at Apatity, Oulu, and South Pole NMs during the initial phase of the event. These three polar NM stations responded to fluxes with small pitch angles as their asymptotic cones were close to the heliospheric magnetic field (HMF) that was well connected to the eruption core. Applying the techniques described above we obtained the spectral and anisotropy characteristics of the solar particles with a time resolution of 10 min. Figure 4 (left) demonstrates the derived rigidity spectrum during the early phase, while Figure 4 (right) corresponds to the late phase of the event. One can see that the spectrum gradually softened throughout the event. The steepening of the spectrum during the early phase was moderate, while it was weak in the late phase. The corresponding fluence (integrated flux over the pitch angle and time) for two periods of the event is presented in Figure 5. The derived pitch angle distribution reveals two peaks and broadens gradually throughout the event (Figures 6 and 7). The spectral and anisotropy characteristics are summarized in Table 1.

The accuracy of the derived GLE characteristics is about 5–8%. Here we use a conservative approach to the accuracy, i.e., the maximum residual of the derived final solution [*More et al.*, 1980]. The construction of the covariance matrix in this case is quite sensitive, since it is dependent on the proximity of the solution to the local minimum. Therefore, the stopping criteria of the inverse problem solution are based mostly on the residual viz., actual and predicted relative reductions in the sum of squared residuals and relative errors between two consecutive iterations [*Aster et al.*, 2012; *Dennis and Schnabel*, 1996]. The accuracy of the estimation of the apparent source direction (geographic latitude and longitude) depends on the particle anisotropy as well as on the asymptotic direction of the considered NM stations. It changes throughout the event. The uncertainty

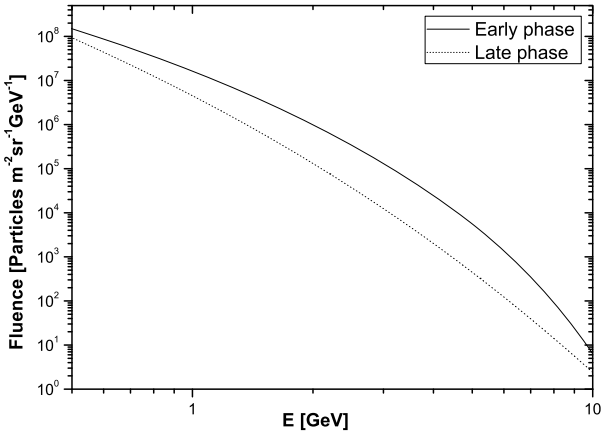

Figure 5. Angle-averaged proton fluence of GLE 71 for two phases of the event. The fluence for the early phase is integrated for 02:00–02:40 UT, while the fluence for the late phase is integrated for 02:40–03:20 UT.

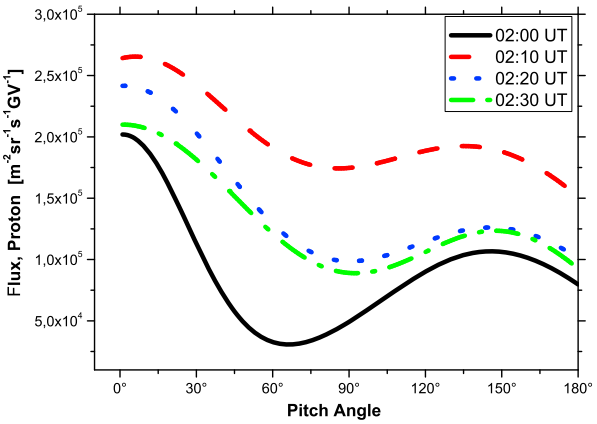

Figure 6. Derived pitch angle distribution of high-energy SEPs during early phase of GLE 71 for 10 min intervals. The flux is given for 1 GV rigidity, assuming constant shape as function of the rigidity. Time (UT) refers to the start of the corresponding 10 min interval.

increases as particle flux declines. The derived apparent source direction is not far from the direction of the IMF near Earth (Figures 2 and 3). Figure 8 shows a comparison of the observed and calculated relative increases at stations with maximum responses as well as at several stations with moderate responses throughout the event. A good agreement is achieved. Similar agreement between the observed and calculated fractional increase is achieved for all other NMs.

The derived angular distribution reveals two peaks. The main peak at $\alpha \approx 0°–30°$ is the direct particle stream along the interplanetary magnetic field line from the Sun. The second, counterstreaming flux peaks at $\alpha \approx 120°–150°$. The event is most likely observed inside a large-scale interplanetary magnetic field structure of an old coronal mass ejection. There are several remote and in situ indications that late in the day of 16 May 2012, the Earth had entered an interplanetary structure of a previous coronal mass ejection (ICME) and stayed inside for about 1 day. That CME was launched from the Sun toward the Earth at around 23:40 UT on 11 May with the speed of only $\approx$ 370 km s^{-1} arriving at the Earth at around 16:30 UT on 16 May 2012, according to the lateral observations of the HI-1 telescope of the Sun-Earth Connection Coronal and Heliospheric Investigation (SECCHI) on the *STEREO A* spacecraft situated about 115° west from the Earth. From the expected ICME arrival time onward, in situ plasma and magnetic field instruments onboard ACE registered the ICME signatures as a gradual increase of magnetic field intensity, slow rotation of the magnetic field vector, and decrease of the proton temperature. The old CME results in an unusual structure of the interplanetary magnetic field. It could affect the particle transport conditions and hence the angular distribution of high-energy particles arriving from the new and fast CME of 17 May 2012.

In application to the 22 October 1989 GLE, *Ruffolo et al.* [2006] considered two types of the interplanetary magnetic field structure that might be associated with a previous CME and could affect the directional distribution of solar protons around the Earth: (i) draping of open interplanetary magnetic field lines around the CME edge, forming a magnetic bottleneck configuration near the Earth and (ii) a closed magnetic loop of the CME itself extending from the Sun to the Earth, as illustrated by their Figure 7. The first suggestion implies a loss cone-type feature in the proton distribution in the antisunward hemisphere, which would be similar to our distribution shown in Figure 6 if we had no particles arriving exactly from antisunward direction, $\alpha = 180°$. In application to the 2 May 1998 event, *Kocharov et al.* [2005] proposed a mixed magnetic configuration suggesting that the bottleneck was formed in a section of closed magnetic loop of the previous CME, with an opportunity to inject solar particles either to one or to both foot points (legs) of the loop and reflect some of the particles at the bottleneck near the Earth's orbit.

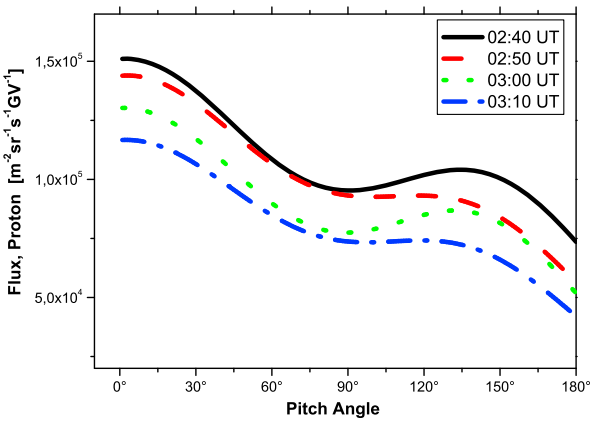

Figure 7. Derived pitch angle distribution of high-energy SEPs during main and late phase of GLE 71 for 10 min intervals. The flux is given for 1 GV rigidity, assuming constant shape as function of the rigidity. Time (UT) refers to the start of the corresponding 10 min interval.

We have applied a previous numerical model [*Kocharov et al.*, 2005, 2007] to the analysis of the high-energy proton

Table 1. Reconstructed Spectra and Axis of Anisotropy of GLE 71[a]

Time UT	J_0 (m^{-2} s^{-1} sr^{-1} GV^{-1})	γ	$\delta\gamma$	σ_1^2 (rad^2)	B	σ_2^2 [Rad^2]	α' (Rad)	Ψ (Deg)	Λ (Deg)
02:00	201,385	−3.63	0.3	0.42	0.53	1.21	2.53	−21.44	51.59
02:10	251,800	−4.69	0.68	1.35	0.75	2.17	2.43	−23.51	63.70
02:20	239,980	−5.53	0.6	1.25	0.52	1.51	2.56	−8.71	64.5
02:30	209,857	−6.62	0.2	1.67	0.57	1.01	2.61	−6.7	58.39
02:40	146,135	−6.9	0.1	2.01	0.64	1.38	2.5	−10.5	49.2
02:50	142,500	−7.07	0.07	2.05	0.57	1.4	2.39	−10.5	41.2
03:00	130,000	−7.2	0.06	2.1	0.63	1.05	2.45	−5.7	35.1
03:10	118,000	−7.4	0.001	2.3	0.55	1.25	2.38	−5.8	32.0

[a]Time (UT) refers to the start of the corresponding 10 min interval.

distribution inferred from the neutron monitor data of 17 May 2012. The model is able to reproduce a double-peak distribution of protons over their pitch angle, with the maxima caused by directly arriving solar particles at $\alpha \approx 0°$ and by bounced particles at $\alpha \approx 130°$, assuming a large mean-free path and a bottleneck with the magnetic ratio $\approx$ 4 at heliocentric distances from 0.9 to 1.2 AU. However, in such a case the loss

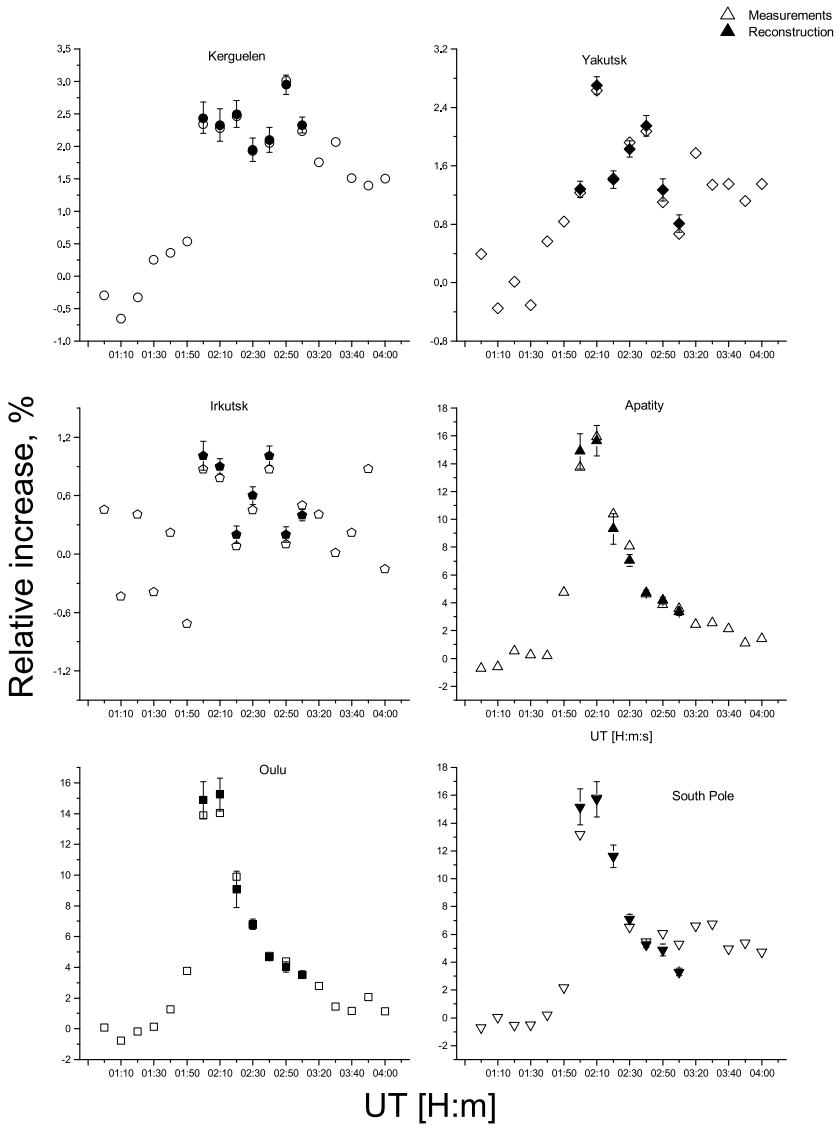

Figure 8. Modeled and observed count rate increases of six NM stations during the GLE on 17 May 2012. The quality of the modeled responses for other stations is of the same order.

cone should be empty, i.e., no particles should arrive from the anti-Sun direction ($\alpha \approx 180°$), which slightly disagrees with the pitch angle distribution derived here from the NM data. However, the nonempty loss cone can be an artifact of the assumed shape of pitch angle distribution (equation (3)). On the other hand, some additional injection along the second leg of the loop could fill the gap up to a level depending on the assumed rate of the second injection, which would be similar to the assumptions by *Ruffolo et al.* [2006] for the GLE of 22 October 1989.

4. Conclusions

We have applied an improved inverse method to analyze neutron monitor observations of the first GLE of solar cycle 24. The comprehensive data set includes counting rate profiles of 21 neutron monitors, which are broadly distributed over the globe and thus cover a wide range of particle arrival directions and a range of geomagnetic cutoff rigidities. This allows derivation of the spectral and angular characteristics of the high-energy particles arriving from the Sun.

The method consists of determining the asymptotic viewing cones of the NM stations with computation of particle trajectories in a model magnetosphere and solving of the inverse nonlinear problem for fitting the world NM network response. Asymptotic viewing directions are calculated for the locations of the neutron monitors using the IGRF and Tsyganenko 1989 magnetospheric field models. Modeling of NM responses is performed using the recently published NM yield function. We employ a modified power law rigidity spectrum of solar particles and superposition of two Gaussians for their pitch angle distribution. Compared with previous analyses, the more general pitch angle formalism allows more realistic interpretation of the local characteristics of the particle propagation. The time evolution of the particle pitch angle distribution is demonstrated in the included supporting information.

The 17 May 2012 event has revealed a very anisotropic onset observed as a sudden intensity increase at only three neutron monitor stations. The inferred pitch angle distribution reveals a second stream at 120–150° apart from the main flux direction. This loss cone-type feature is indicative of a nonstandard mode of the particle propagation and could be caused by an interplanetary magnetic field structure associated with a previous CME. The results presented here expands the studies of the GLE on 17 May 2012 [e.g., *Li et al.*, 2013].

Further improvement of the method is possible, namely, extension to a range of spectral forms and pitch angle distributions. However, more complicated spectral shapes or superposition of several spectral shapes, as well as more complicated pitch angle distribution function would require more free parameters leading to less robust results.

Acknowledgments

The authors acknowledge NMDB and all our colleagues from the neutron monitor stations, who kindly provided the data used in this analysis. The data are acquired from the following stations: Alma Ata, Apatity, Baksan, Fort Smith, Inuvik, Irkutsk, Jungfraujoch, Kerguelen, Kiel, Magadan, McMurdo, Moscow, Norilsk, Oulu (our data), Rome, South Pole, Terre Adelie, Thule, Tsumeb, Tixie Bay, and Yakutsk. Data from Oulu NM is easily available at http://cosmicrays.oulu.fi. The authors warmly acknowledge E. Vashenuyk and Yu. Balabin from Polar Geophysical Institute of Russian Academy of Sciences for discussions concerning GLE analysis methodology. The research leading to these results has received funding from the European Union's Seventh Framework Programme (FP7/2007-2013) under grant agreement 262773 (SEPServer) and from Academy of Finland (project 260596).

Philippa Browning thanks Marcus Duldig and an anonymous reviewer for their assistance in evaluating this paper.

References

Agostinelli, S., J. Allison, and K. Amako (2003), Geant4—A simulation toolkit, *Nucl. Instrum. Methods Phys. Res., Sect. A*, *506*(3), 250–303.

Aschwanden, M. (2012), GeV particle acceleration in solar flares and ground level enhancement (GLE) events, *Space Sci. Rev.*, *171*(1-4), 3–21.

Aster, R., B. Borchers, and C. Thurber (2012), *Parameter Estimation and Inverse Problems*, Elsevier Academic Press, Burlington, Mass.

Bazilevskaya, G. A., et al. (2008), Cosmic ray induced ion production in the atmosphere, *Space Sci. Rev.*, *137*, 149–173.

Bieber, J., and P. Evenson (1995), Spaceship Earth—An optimized network of neutron monitors, in *Proc. of 24th International Cosmic Ray Conference*, vol. 4, edited by N. Iucci and E. Lamanna, pp. 1316–1319, International Union of Pure and Applied Physics, Rome, Italy.

Bieber, J., W. Droge, P. Evenson, K. Pyle, D. Ruffolo, U. Pinsook, P. Tooprakai, M. Rujiwarodom, T. Khumlumlert, and S. Krucker (2002), Energetic particle observations during the 2000 July 14 solar event, *Astrophys. J.*, *567*(1), 622–634.

Bombardieri, D., M. Duldig, K. Michael, and J. Humble (2006), Relativistic proton production during the 2000 July 14 solar event: The case for multiple source mechanisms, *Astrophys. J.*, *644*(1), 565–574.

Burger, R., M. Potgieter, and B. Heber (2000), Rigidity dependence of cosmic ray proton latitudinal gradients measured by the ulysses spacecraft: Implication for the diffusion tensor, *J. Geophys. Res.*, *105*, 27,447–27,445.

Buetikofer, R., E. Flueckiger, L. Desorgher, and M. Moser (2008), The extreme solar cosmic ray particle event on 20 January 2005 and its influence on the radiation dose rate at aircraft altitude, *Sci. Total Environ.*, *391*(2-3), 177–183.

Caballero-Lopez, R., and H. Moraal (2004), Limitations of the force field equation to describe cosmic ray modulation, *J. Geophys. Res.*, *109*, A01101, doi:10.1029/2003JA010098.

Clem, J. (1997), Contribution of obliquely incident particles to neutron monitor counting rate, *J. Geophys. Res.*, *102*, 26,919–26,926.

Cliver, E., S. Kahler, and D. Reames (2004), Coronal shocks and solar energetic proton events, *Astrophys. J.*, *605*, 902–910.

Cooke, D., J. Humble, M. Shea, D. Smart, N. Lund, I. Rasmussen, B. Byrnak, P. Goret, and N. Petrou (1991), On cosmic-ray cutoff terminology, *Il Nuovo Cimento C*, *14*(3), 213–234.

Cramp, J., J. Humble, and M. Duldig (1994), The cosmic ray ground-level enhancement of 24 October 1989, *Proc. Astr. Soc. Aust.*, *11*(1), 28–32.

Cramp, J., M. Duldig, E. Flueckiger, J. Humble, M. Shea, and D. Smart (1997), The October 22, 1989, solar cosmic ray enhancement: An analysis the anisotropy spectral characteristics, *J. Geophys. Res.*, *102*(A11), 24,237–24,248.

Debrunner, H., E. Flueckiger, H. Graedel, J. Lockwood, and R. McGuire (1988), Observations related to the acceleration, injection, and interplanetary propagation of energetic protons during the solar cosmic ray event on February 16, 1984, *J. Geophys. Res.*, *93*(A7), 7206–7216.

Dennis, J., and R. Schnabel (1996), *Numerical Methods for Unconstrained Optimization and Nonlinear Equations*, Prentice-Hall, Englewood Cliffs, N. J.

Desorgher, L., E. Flueckiger, M. Gurtner, M. Moser, and R. Buetikofer (2005), A Geant 4 code for computing the interaction of cosmic rays with the Earth's atmosphere, *Int. J. of Mod. Phys. A*, *20*(A11), 6802–6804.

Dorman, L. (2004), *Cosmic Rays in the Earth's Atmosphere and Underground*, Kluwer Academic Publishers, Dordrecht, Netherlands.

Dorman, L. (2006), *Cosmic Ray Interactions, Propagation, and Acceleration in Space Plasmas, Astrophysics and Space Science Library 339*, Springer, Dordrecht.

Gleeson, L., and W. Axford (1968), Solar modulation of galactic cosmic rays, *Astrophys. J.*, *154*, 1011–1026.

Hatton, C. (1971), *The Neutron Monitor, Progress in Elementary Particle and Cosmic-Ray Physics X*, chap. 1, North Holland Publishing Co., Amsterdam.

Kocharov, L., G. Kovaltsov, J. Torsti, and K. Huttunen-Heikinmaa (2005), Modeling the solar energetic particle events in closed structures of interplanetary magnetic field, *J. Geophys. Res.*, *110*, A12S03, doi:10.1029/2005JA011082.

Kocharov, L., O. Saloniemi, J. Torsti, G. Kovaltsov, and E. Riihonen (2007), Scanning an interplanetary magnetic cloud using high-energy protons, *Astrophys. J.*, *654*(2), 1121–1127.

Kudela, K., and I. Usoskin (2004), On magnetospheric transmissivity of cosmic rays, *Czech. J. Phys.*, *54*(2), 239–254.

Kudela, K., R. Bučik, and P. Bobik (2008), On transmissivity of low energy cosmic rays in disturbed magnetosphere, *Adv. Space Res.*, *42*(7), 1300–1306.

Langel, R. (1987), Main field in geomagnetism, in *Geomagnetism*, edited by J. A. Jacobs, chap. 1, pp. 249–512, Academic Press, London.

Levenberg, K. (1944), A method for the solution of certain non-linear problems in least squares, *Quart. Appl. Math.*, *2*, 164–168.

Li, C., K. A. Firoz, L. P. Sun, and L. I. Miroshnichenko (2013), Electron and proton acceleration during the first ground level enhancement event of solar cycle 24, *Astrophys. J.*, *707*(1), 34.

Marquardt, D. (1963), An algorithm for least-squares estimation of nonlinear parameters, *SIAM J. Appl. Math.*, *11*(2), 431–441.

Mavromichalaki, H., et al. (2011), Applications and usage of the real-time neutron monitor database, *Adv. Space Res.*, *47*, 2210–2222.

McCracken, K. (1962), The cosmic ray are effect: 1. Some new methods for analysis, *J. Geophys. Res.*, *67*, 423–434.

McCracken, K., V. Rao, and M. Shea (1962), The trajectories of cosmic rays in a high degree simulation of the geomagnetic field, *Technical Report 77*, Massachusetts Institute of Technology, Cambridge, Mass.

McCracken, K., V. Rao, B. Fowler, M. Shea, and D. Smart (1968), Cosmic ray tables (asymptotic directions, etc.), in *Annals of the IQSY,* chap. 1, pp. 198–214, MIT Press, Cambridge, Mass.

McCracken, K., F. McDonald, J. Beer, G. Raisbeck, and F. Yiou (2004), A phenomenological study of the long-term cosmic ray modulation, 850–1958 AD, *J. Geophys. Res.*, *109*, A12103, doi:10.1029/2004JA010685.

Mishev, A., and I. Usoskin (2013), Computations of cosmic ray propagation in the Earth's atmosphere, towards a GLE analysis, *J. Phys. Conf. Ser.*, *409*, 012152, doi:10.1088/1742-6596/409/1/012152.

Mishev, A., I. Usoskin, and G. Kovaltsov (2013), Neutron monitor yield function: New improved computations, *J. Geophys. Res. Space Phys.*, *118*, 2783–2788, doi:10.1002/jgra.50325.

More, G., B. Garbow, and K. Hillstrom (1980), User guide for minpack-1, *Report ANL 80-74*, Argonne National Laboratory, Downers Grove Township, Ill.

Nevalainen, J., I. Usoskin, and A. Mishev (2013), Eccentric dipole approximation of the geomagnetic field: Application to cosmic ray computations, *Adv. Space Res.*, *52*(1), 22–29.

Rao, U. R., K. G. McCracken, and D. Venkatesan (1963), Asymptotic cones of acceptance and their use in the study of the daily variation of cosmic radiation, *J. Geophys. Res.*, *68*(2), 345–369.

Reames, D. (1999), Particle acceleration at the Sun and in the heliosphere, *Space Sci. Rev.*, *90*(3-4), 413–491.

Ruffolo, D., P. Tooprakai, M. Rujiwarodom, T. Khumlumlert, M. Wechakama, J. Bieber, P. Evenson, and K. Pyle (2006), Relativistic solar protons on 1989 October 22: Injection and transport along both legs of a closed interplanetary magnetic loop, *Astrophys. J.*, *639*(2), 1186–1205.

Saiz, A., D. Ruffolo, J. Bieber, P. Evenson, and R. Pyle (2008), Anisotropy signatures of solar energetic particles transport in a closed interplanetary magnetic loop, *Astrophys. J.*, *672*(1), 650–658.

Shea, M., and D. Smart (1982), Possible evidence for a rigidity-dependent release of relativistic protons from the solar corona, *Space Sci. Rev.*, *32*, 251–271.

Shea, M., and D. Smart (1990), A summary of major solar proton events, *Sol. Phys.*, *127*, 297–320.

Shea, M., D. Smart, J. E. Humble, E. O. Flueckiger, L. C. Gentile, and M. R. Nichol (1987), A revised standard format for cosmic ray ground-level event data, paper presented at 20th ICRC, Moscow.

Shea, M., D. Smart, and K. McCracken (1965), A study of vertical cut off rigidities using sixth degree simulations of the geomagnetic field, *J. Geophys. Res.*, *70*, 4117–4130.

Simpson, J., W. Fonger, and S. Treiman (1953), Cosmic radiation intensity-time variation and their origin. I. Neutron intensity variation method and meteorological factors, *Phys. Rev.*, *90*, 934–950.

Smart, D., M. Shea, and E. Fluckiger (2000), Magnetospheric models and trajectory computations, *Space Sci. Rev.*, *93*(1), 305–333.

Tsyganenko, N. (1989), A magnetospheric magnetic field model with a warped tail current sheet, *Planet. Space Sci.*, *37*(1), 5–20.

Usoskin, I., and G. Kovaltsov (2006), Cosmic ray induced ionization in the atmosphere: Full modeling and practical applications, *J. Geophys. Res.*, *111*, D21206, doi:10.1029/2006JD007150.

Usoskin, I., K. Alanko-Huotari, G. Kovaltsov, and K. Mursula (2005), Heliospheric modulation of cosmic rays: Monthly reconstruction for 1951–2004, *J. Geophys. Res.*, *110*, A12108, doi:10.1029/2005JA011250.

Usoskin, I., G. Bazilevskaya, and G. A. Kovaltsov (2011), Solar modulation parameter for cosmic rays since 1936 reconstructed from ground-based neutron monitors and ionization chambers, *J. Geophys. Res.*, *116*, A02104, doi:10.1029/2010JA016105.

Vashenyuk, E., Y. Balabin, J. Perez-Peraza, A. Gallegos-Cruz, and L. Miroshnichenko (2006), Some features of the sources of relativistic particles at the Sun in the solar cycles 21–23, *Adv. Space. Res.*, *38*(3), 411–417.

Vashenyuk, E., Y. Balabin, B. Gvozdevsky, and L. Schur (2008), Characteristics of relativistic solar cosmic rays during the event of December 13, 2006, *Geomag. Aeron.*, *48*(2), 149–153.